TWO-DIMENSIONAL FLOW ANALYSIS OF MONGLA RIVER USING HEC-RAS

Md. Arafat Rahman Pranto[1], Md. Shahjahan Ali[2], M. Mubtasim Fuad Dip[*3], Mehedy Hasan Munna[4], and Md. Motiur Rahman[5]

[1] *Undergraduate Student, Department of Civil Engineering, Khulna University of Engineering and Technology, Bangladesh, e-mail: arafatrahman337@gmail.com*
[2] *Professor, Department of Civil Engineering, Khulna University of Engineering and Technology, Bangladesh, e-mail: msali@ce.kuet.ac.bd*
[3] *Lecturer, Department of Civil Engineering, Khulna University of Engineering and Technology, Bangladesh, e-mail: dip@ce.kuet.ac.bd*
[4] *Undergraduate Student, Department of Civil Engineering, Khulna University of Engineering and Technology, Bangladesh, e-mail: mehedyhasan3030@gmail.com*
[5] *Executive Engineer, Mongla Port Authority, Bagerhat, Bangladesh, e-mail: khan.motiur06@gmail.com*

***Corresponding Author**

ABSTRACT

This study presents a two-dimensional hydrodynamic analysis of the Mongla River, Bangladesh, using the HEC-RAS 2D model driven by 2019 hydrological and bathymetric data. Calibration against observed water levels produced an overall correlation coefficient of 0.75, with markedly higher accuracy during the high-flow season (R^2 up to 0.95). Results indicate a semi-diurnal, tide-dominated system with strong seasonal variability, characterized by tidal damping (0.91–1.0 in the high-flow season and 0.81–0.87 in the low-flow season) and a consistent upstream–downstream phase lag of 2–2.5 hours. Peak water levels declined from 3.93 mPWD upstream to 3.46 mPWD downstream, reflecting progressive energy dissipation, while velocities ranged from 0.92 to 2.5 m/s. A distinct convergence zone near chainage 11 km was identified, where opposing tidal flows reduce velocity and enhance sediment deposition potential. Discharge analysis revealed persistent flood-tide dominance, with maximum asymmetry (47%) occurring during the high-flow spring tide. Comparison with Delft3D showed strong agreement (R^2 = 0.97–0.99), confirming the robustness of HEC-RAS 2D for tidal river simulations. By integrating tidal amplification, damping, phase shifts, velocity fields, and discharge asymmetry, the study improves understanding of the hydrodynamic processes driving chronic siltation and navigability loss in the Mongla River. Although limited by single-year simulations and the absence of explicit sediment transport modeling, the findings provide practical guidance for targeted dredging, navigation maintenance, and adaptive river management, demonstrating the value of two-dimensional hydrodynamic modeling for tide-dominated deltaic rivers.

Keywords: *Tidal River, Tidal Amplification & Damping, Phase Shift, Spring Tide, Neap Tide*

1. INTRODUCTION

Rivers are open geomorphic systems, which involve the movement of water and sediment, as well as the transportation of nutrients, and they continuously change their morphology based on boundary conditions. In tide-dominated deltas, hydrodynamics and sediment transportation are subject to control by the interaction of river discharge and tidal forcing, giving rise to complex spatial and temporal variability (Rahman & Ali, 2024). Bangladesh is one of the most active deltaic settings in the world, with a rich network of fluvial systems that also hosts 57 transboundary systems that are found in both India and Myanmar (River and Delta Research Centre, 2023). In the Ganges Brahmaputra Meghna (GBM) delta, interconnected river estuary systems produce a high degree of variability in flow velocity, intrusion of salinity, and erosion-deposition across exceptionally high sediment loads due to monsoon flows and extremely high sediment loads.
The Mongla River in Southwest Bangladesh forms a vital part of this network of deltas (Figure 1). It sustains a UNESCO World Heritage site, the Sundarbans mangrove ecosystem, and serves as a main navigation route between the Mongla Port and Khulna and inland waterways. Due to its direct interrelationship with the Bay of Bengal, the river shows very high tidal variation of water levels and velocities. In the past decades, however, navigability has been damaged because of sedimentation, tidal pumping, decreased tidal prism, polders, and the blocking of natural drainage systems. Although dredging was repeated and other canal excavation works had been carried out before, channel capacity is still limited by rapid infill, which is reported to occur to the level of near-complete channel resiltation in 30-40 days (Rahman et al., 2013), interfering with the channel functioning and security of ship movements.

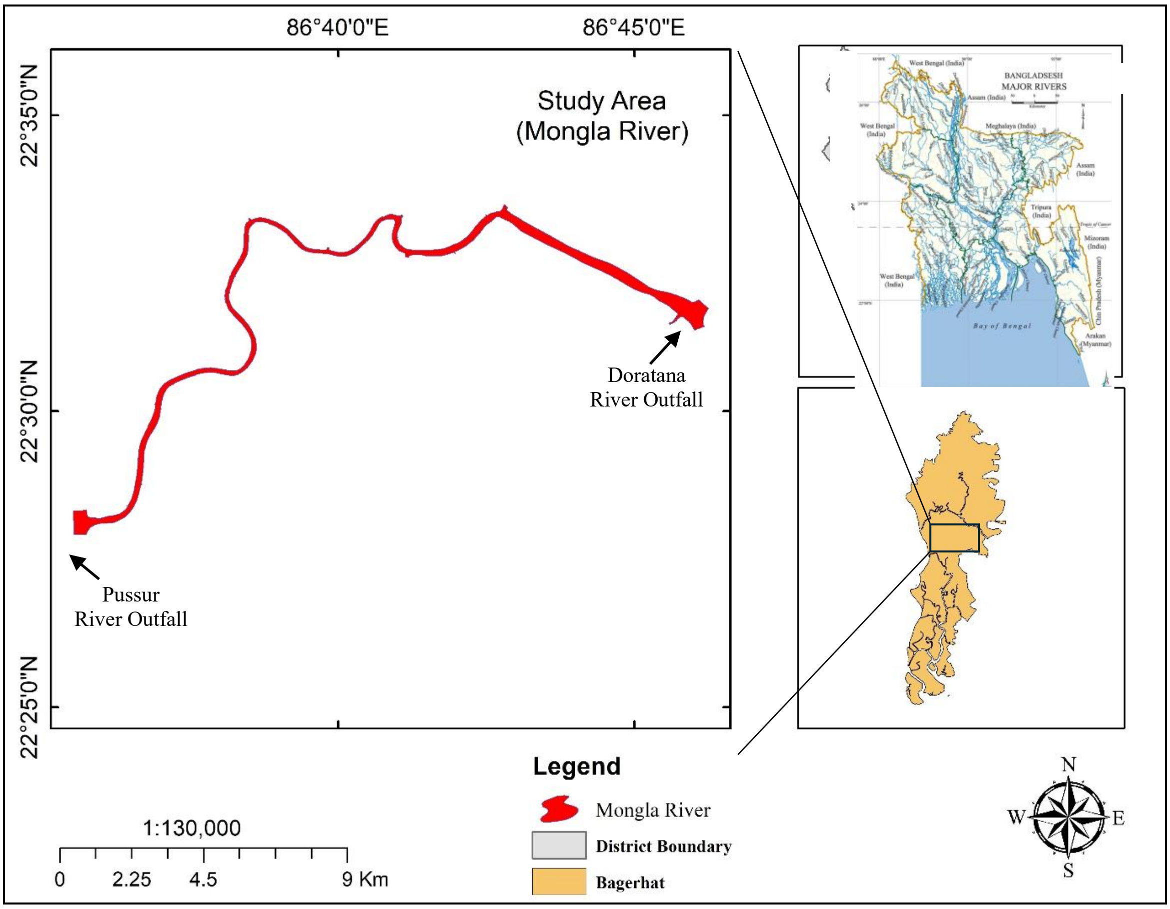

Figure 1: Study reach of the Mongla River

Previous research determined that tidal processes exert one of the major impacts on the channel morphology and on the channel sediment dynamics in the deltaic rivers. Hoitink and Jay (2016) showed that the nonlinear interplay of the tidal processes regulates the processes of sediment import as well as export, and Hoitink et al. (2017) highlighted the stabilizing impact of tidal energy on channel networks of tide-driven deltas, such as the Ganges-Brahmaputra-Meghna (GBM) system. Other estuarine systems in which numerical modelling is used to study the effect of tidal amplification, wave-current interactions, and sea-level rise on hydrodynamic behavior include the Columbia River system (Savant et al., 2014) and the Elbe estuary (Mahavadi et al., 2024). In Bangladesh, the problem of tidal asymmetry, sedimentation, and low navigability is invariably identified as the most crucial management challenge in hydrodynamic studies of the rivers Pussur, Sibsa, Meghna, and Karnafuli (Alam et al., 2014; Kabir and Ali, 2017; Rahman and Ali, 2018). Regardless of these contributions, the Mongla River has not been studied systematically using the modern two-dimensional numerical modelling frameworks.

Also, two-dimensional (2D) dynamic models are becoming more popular in riverine and estuarine systems, due to their ability to solve the variability of lateral flows without losing computational efficiency (Ali, 2008). Recent inter-model comparison research studies have highlighted the need to have a rigorous level of performance assessment in order to choose models. A review of five common 2D models by Samir (2024) revealed that Delft3D and SRH-2D exhibited superior fidelity in capturing expected conditions of rivers, with Delft3D also showing great computational efficiency. Similarly, Munoz et al. (2021) noted that Delft3D-FM was superior to HEC-RAS 2D in coastal-estuarine system contexts when atmospheric forcing occurred, but HEC-RAS 2D remained a viable alternative in systems where riverine and tidal processes were predominant.

Through these developments, there are still major gaps in the existing literature. Most of the inter-model comparisons are focused on flood aspects and not on tidal or annual flow regimes, and few studies focus on tropical deltaic ecosystems like the GBM. Moreover, the sensitivity of 2D model performance to bathymetric representation, roughness parameterization, and mesh configuration has not been properly studied in upstream tidal rivers. Furthermore, a study has not provided a comprehensive 2D hydrodynamic characterization of the Mongla River or been in a position to examine the caliber of the highly accessible platform, like HEC-RAS 2D, in the context of this system. This lack of specific analysis impedes the development of evidence-based methods for navigation maintenance and sediment management.

To overcome these drawbacks, the paper will develop a hydrodynamic model of the Mongla River, using the HEC-RAS 2D mathematics, to measure tidal propagation properties, such as amplification, lag, and spatial distribution of velocity and discharge, along a portion of the river, between Doratana and the Pussur River confluence. The study provides a process-based analysis of tidal processes in a data-poor, tide-dominated river system through the combination of field measurements, high-resolution bathymetries, and numerically constrained process simulations. The results are supposed to be used in navigation planning and sediment operationalization, and they are supposed to form a foundation for new model comparisons of Delft3D with other modern hydrodynamic operational frameworks.

2. METHODOLOGY

This study applied a combined numerical modeling approach using HEC-RAS 2D and Delft3D Flexible Mesh (FM) to simulate the hydrodynamic behavior of the Mongla River. The workflow began with data collection and preprocessing, which formed the foundation for model development, calibration, and validation. Recent bathymetry, discharge, and water-level data were obtained from the Mongla Port Authority (MPA) and the Bangladesh Water Development Board (BWDB). Bathymetric data were processed in ArcGIS (ArcMap 10.5) to generate a Digital Elevation Model (DEM), which was subsequently used in both modeling platforms.

For the HEC-RAS 2D model (version 6.5), the DEM was imported through RAS Mapper to define the computational domain between the Doratana and Pussur River outfalls. A two-dimensional flow area was delineated, and a computational mesh comprising 19,762 cells with a uniform resolution of 15 m × 15 m was generated. Mesh sensitivity analysis demonstrated that finer grid resolutions significantly increased computational runtime but did not result in statistically meaningful improvements in simulated water levels or velocity fields. Boundary conditions were assigned using 2019 hydrological records, with discharge from Doratana as the upstream input and water-level time series from Pussur as the downstream boundary. The model was configured to solve the Shallow Water Equations (SWE-ELM) with adaptive Courant-based time-step control with a maximum Courant number of 1 and a minimum Courant number of 0.45. After running the unsteady flow simulation, outputs were extracted and analyzed through RAS Mapper.

In parallel, a Delft3D FM model was developed using Delft3D version 1.6.1.47098. The computational grid was generated in RGFGRID by importing the bathymetry and drawing a spline along the river alignment. Grid refinement was applied to achieve a resolution of approximately 25 m, followed by orthogonalization and conversion from a regular to an irregular mesh. The grid was then imported into the FLOW FM interface, where bed levels were interpolated and roughness zones mapped. Upstream discharge (Doratana) and downstream water-level (Pussur) time series were applied as boundary conditions. Model settings were configured by defining the simulation time frame, timestep, and output parameters, including secondary flow processes. Observation points and 15 cross-sections spaced roughly 2 km apart were created for result extraction. After verifying numerical stability, the model was executed, and the results were analyzed across the 2D domain.

Both models were calibrated and validated using observed water-level data at the calibration station (22°28'50.4"N, 89°36'28.7"E). Upon achieving satisfactory agreement between simulated and observed values, the validated HEC-RAS and Delft3D simulations were used to evaluate tidal amplification, damping, velocity distribution, discharge variability, and overall hydrodynamic responses under different tidal phases. Parameters used for 2D hydrodynamic modelling are summarized in Table 1.

Table 1: Summary of Parameters used for 2D Hydrodynamic Model

Parameter	HEC-RAS	Delft3D
Mesh Size	15 m x 15 m	25 m Orthogonal
Manning's n value range	0.008-0.035	0.010-0.035
Optimum n value	0.025	0.030
Equation	SWE-ELM	SWE-ELM

3. RESULTS AND DISCUSSIONS

3.1 Model Calibration

Model calibration and validation were performed using observed water level records to assess the accuracy of both the HEC-RAS 2D and Delft3D FM simulations. For both the HEC-RAS and Delft3D models, calibration was conducted using 2019 water level data at the designated point (22°28'50.4"N, 89°36'28.7"E). For the HEC-RAS model, Manning's n values between 0.008 and 0.035 were tested, with 0.025 yielding the best fit. For the Delft3D model, Manning's n values derived from land-cover data n = 0.010–0.035 were evaluated, and the model showed the strongest regression performance at n = 0.03. The seasonal breakdown of simulated results is presented in Table 2.

Table 2: Statistical evaluation of water level calibration

Season	Statistical Parameter					
	R^2		RSR		NSE	
	HEC-RAS	Delft3D	HEC-RAS	Delft3D	HEC-RAS	Delft3D
LFS-	0.8994	0.9732	0.4360	0.2518	0.8052	0.9324

Spring						
LFS-Neap	0.7937	0.8232	1.0044	1.080	<0.5	<0.5
HFS-Neap	0.9054	0.9881	0.4392	0.2460	0.8022	0.9354
HFS-Spring	0.9499	0.9254	0.3335	0.4044	0.8860	0.8268

The model indicates good performance of HFS-Neap Tide, as shown by the statistical indicators. The regression coefficient ($R^2 = 0.9054$) shows that the consistency between the simulated and observed values is quite strong (Figures 2 and 3), and it shows that the model is successful in terms of capturing a range of variability of the system. The value of Root Mean Standard Deviation Ratio (RSR) of 0.4392 shows low values of Residual errors against observed standard deviation, whereas the Nash-Sutcliffe Efficiency, NSE = 0.9069, indicates good predictive power.

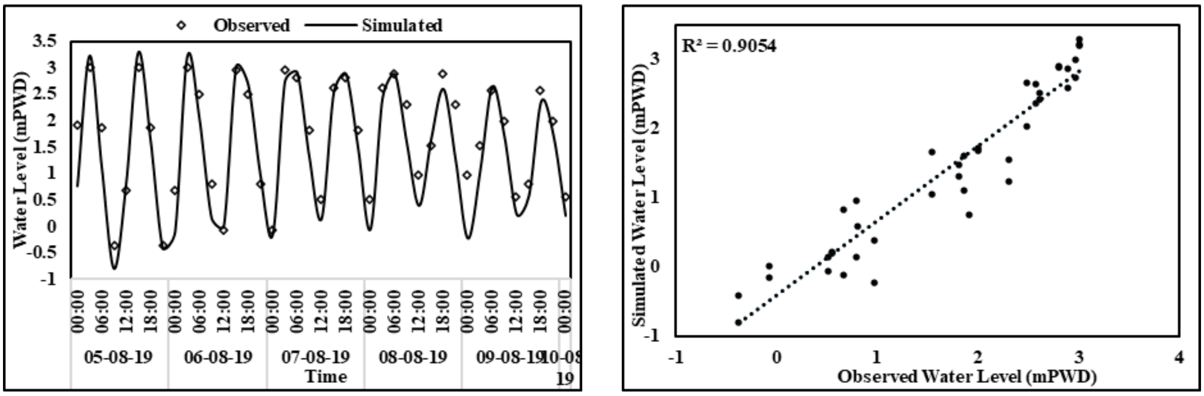

Figure 2: HEC-RAS Model calibration for Water Level for HFS (Neap Tide-Aug 5th to Aug 9th)

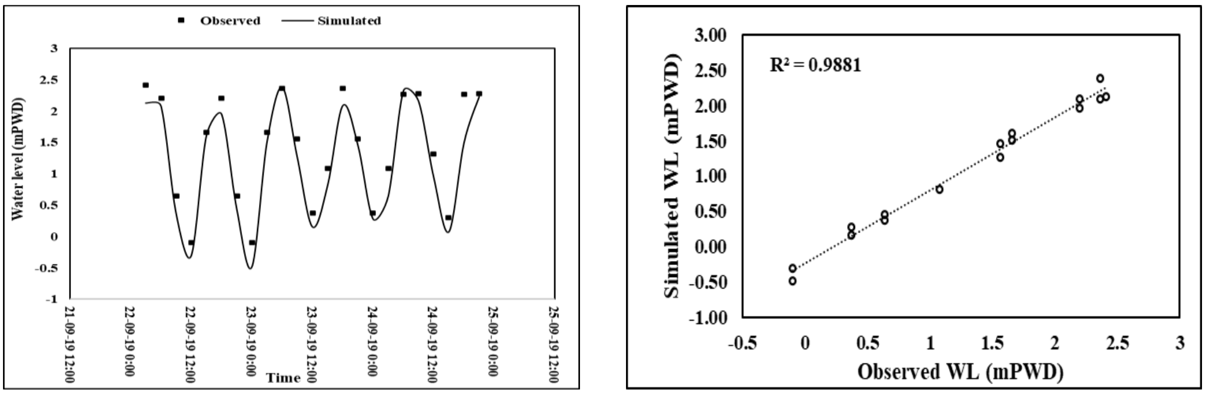

Figure 3: Comparison of simulated and observed WSE for HFS (Neap Tide) for Delft3D Model

Generally, very good results are obtained with the model on HFS-Spring Tide (Figures 4 and 5). Similar to the previous coefficient, the regression ($R^2 = 0.9499$) presents a great deal of correspondence between the simulated and observed values, which demonstrates that the model fits the variability of the system well. Small errors in terms of their residual value are indicated by a low RSR value of 0.3335 with respect to the standard deviation that was recorded. The NashSutcliffe Efficiency (NSE =0.5983) implies that the predictive ability of the model is acceptable; thus, whereas it is effective in relevance to long-term trends and values, it does not explain short-term variations or extreme values.

According to the outcomes of the simulation provided in Figures 6 and 7, the model does not show any problematic behavior. The political aspect of the coefficient of regression (R2 = 0.8994) indicates a high correlation between (simulated) and observed values, which implies that the model has been able to explain the overall variability of the system. The RSR of 0.4360 lies within a range considered to be good in terms of the number of residual errors, which are relatively small, against the standard deviation that was observed. Nevertheless, the NashSutcliffe Efficiency (NSE) of below 0.5 indicates that the model serves a high level of predicting the general trends, but the scale of the prediction of the model is less than ideal in regard to some magnitudes or time changes. This difference is probably due to the imprecision of boundary conditions, spatial uncertainty in roughness, or simplistic modeling of complicated tidal processes.

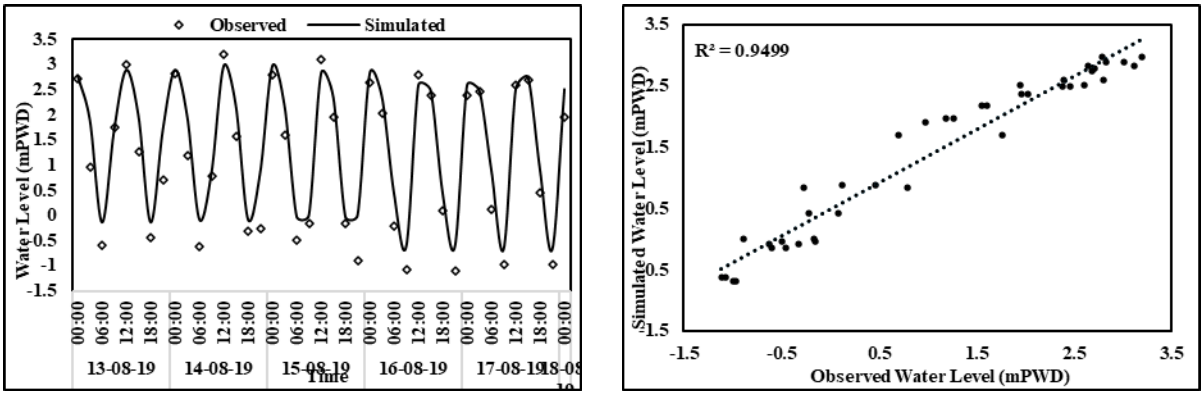

Figure 4: HEC-RAS Model calibration for Water Level for HFS (Spring Tide- Aug 13th to Aug 17th)

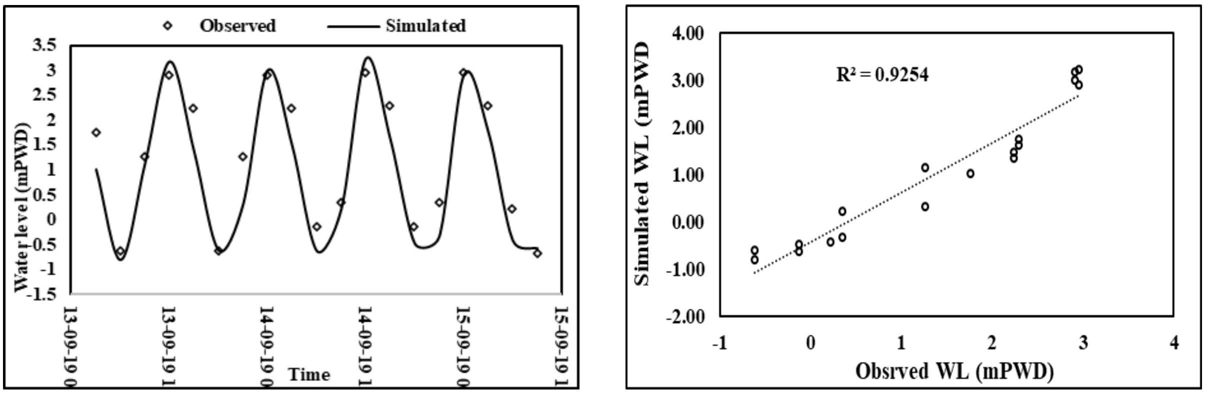

Figure 5: Comparison of simulated and observed WSE for HFS (Spring Tide) for Delft3D Model

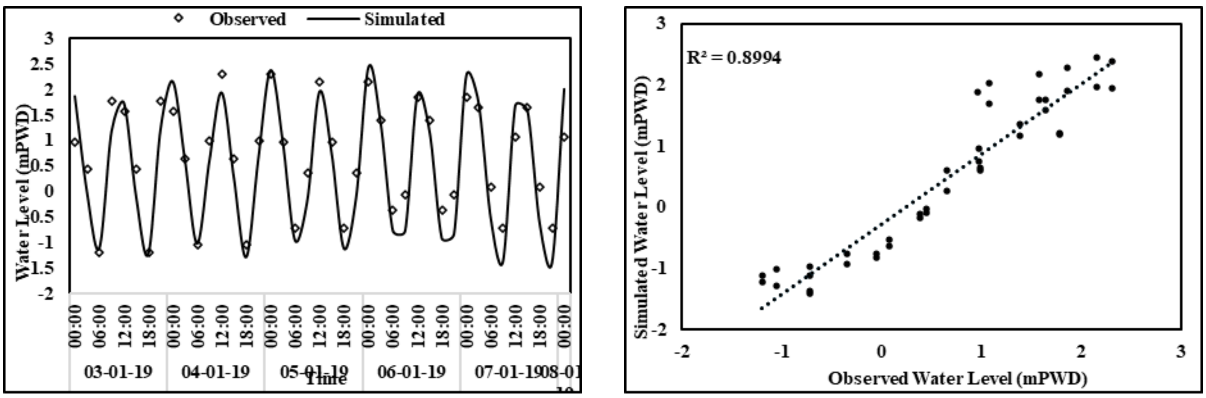

Figure 6: HEC-RAS Model calibration for Water Level for LFS (Spring Tide- Jan 3rd to Jan 7th)

The simulation exhibits a high performance in terms of all the performance (R^2 = 0.7937), where the value is good enough to identify the close relationship between the simulated and the observed values, which ensures that the model fits the major variability of the mechanism (Figures 8 and 9). The RSR of 1.004 indicates a moderate amount of residual error with respect to the measured standard deviation; meanwhile, the Nash-Sutcliffe Efficiency (NSE = 0.9260) is large, which results in the high predictive capability as well as what is deemed to be high-degree reliability in the reproduction of observed dynamics. However, when the river is in low flow season, some major parts of the river reach will partially dry, and it cannot be well captured in the modeling system. The restriction renders the model less successful in modeling extremely shallow/dry conditions, and consequently, its regression coefficient comes out relatively low compared to that of other seasons. In spite of this limitation, it can be argued that the overall performance of the model is satisfactory in terms of understanding the overall hydrodynamic behaviour of the river.

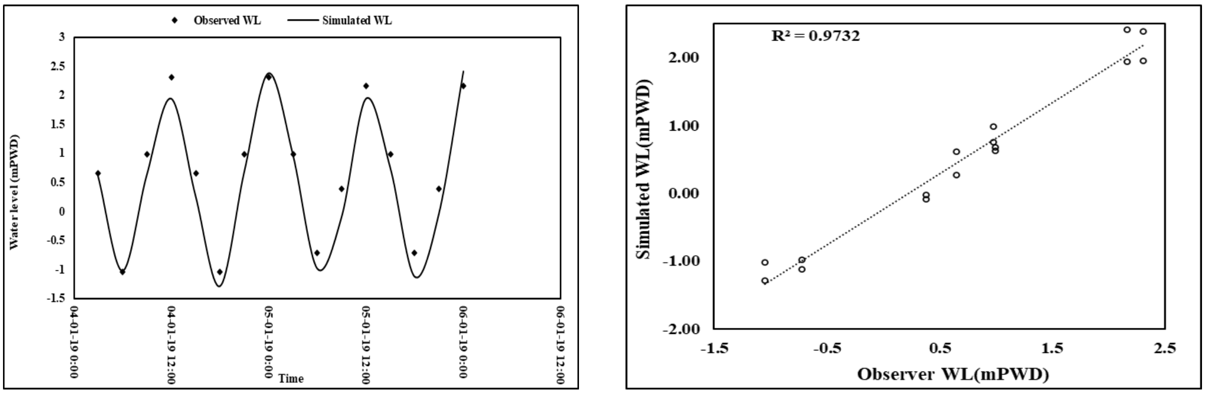

Figure 7: Comparison of simulated and observed WSE for LFS (Spring Tide) for Delft3D

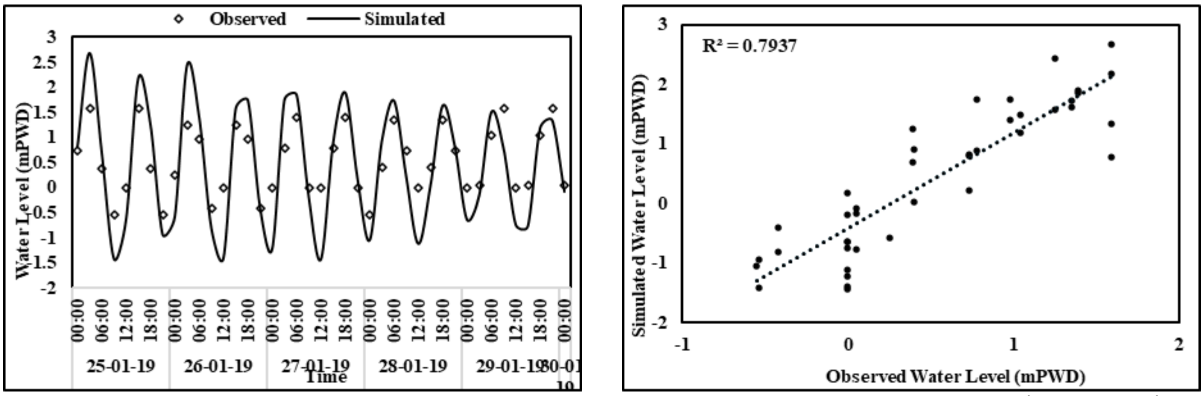

Figure 8: HEC-RAS Model calibration for Water Level for LFS (Neap Tide- Jan 25th to Jan 29th)

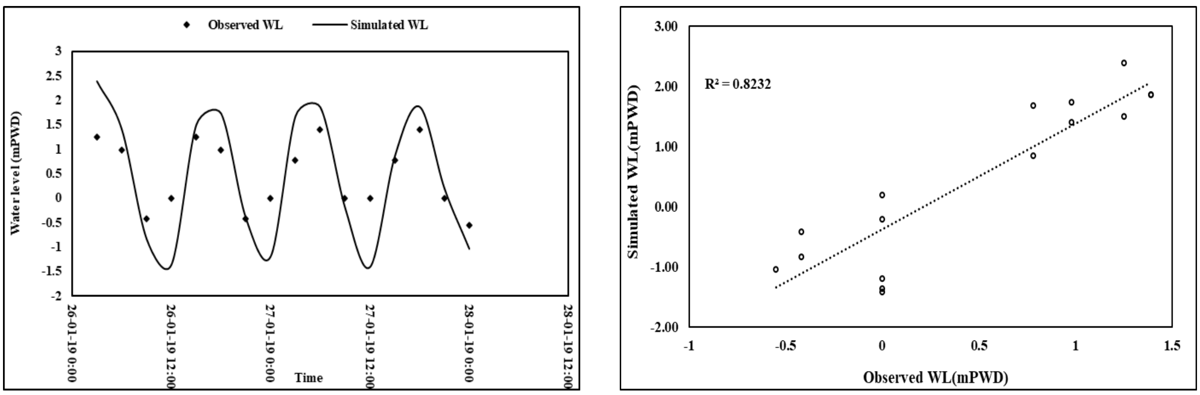

Figure 9: Comparison of simulated and observed WSE for LFS (Neap Tide) for Delft3D

The coefficient of regression (R^2 = 0.7505 for HEC-RAS and R^2=0.7483 for Delft3D) indicates a good level of agreement between simulated and observed values, showing that the model captures the dominant variability of the system (Figures 10 and 11). While some discrepancies remain, this level of correlation is generally considered acceptable for hydrodynamic simulations in complex tidal river environments, supporting the model's suitability for analyzing overall flow behavior and spatial trends.

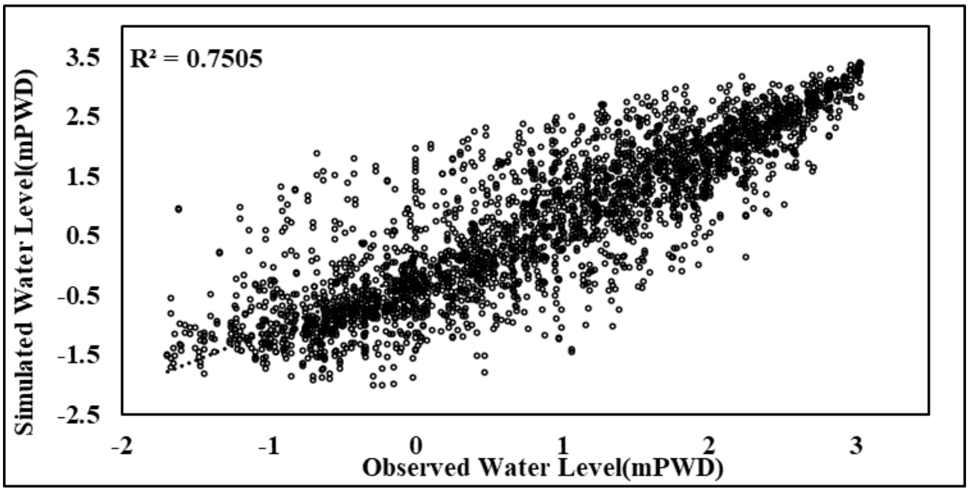

Figure 10: Overall coefficient of correlation for the year 2019 in HEC-RAS

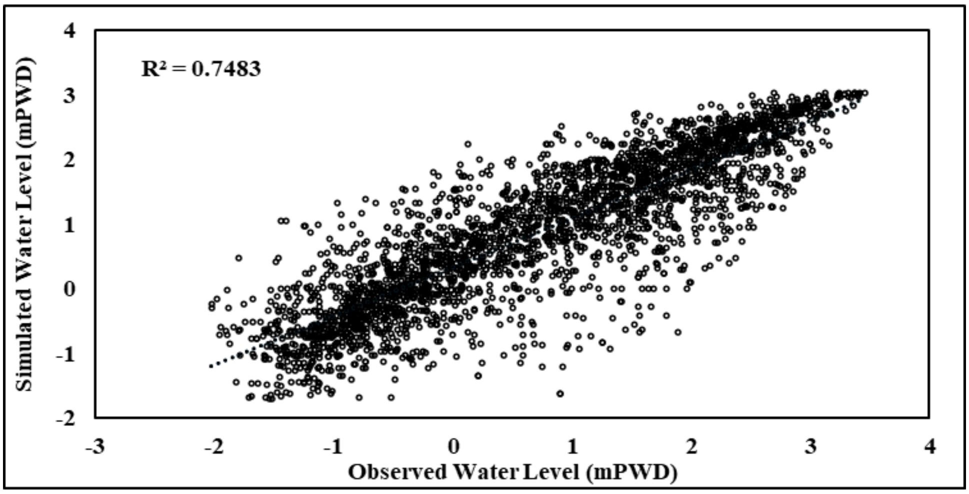

Figure 11: Overall coefficient of correlation for the year 2019 in Delft3D

3.2 Bed Topography of the Study Area

The study reach covers approximately 28.65 km, extending from the Doratana River outfall to the Pussur River outfall. At the mouth, the channel exhibits a width of 262.3 m, a depth of 16.2 mPWD, and a tidal range of 5.03 m (HFS). The longitudinal bed profile (Figure 12) reveals distinct spatial variations in channel depth along the reach. The upstream section, extending up to 9,000 m, is relatively shallow with depths ranging between 4–8 mPWD. The mid-reach, between 9,000 m and 18,000 m, is comparatively deeper, with depths varying from 6–11 mPWD, while the downstream section again becomes shallow. The maximum recorded depth is 24.5 mPWD at approximately 377 m from the upstream boundary. Channel width remains relatively consistent, varying between 250–260 m in the upstream and downstream portions, reaching a maximum of 292 m near chainage 1,000 m. In contrast, the middle reach narrows significantly, with widths typically between 120–170 m and locally reducing to nearly 100 m.

a)

b)

c)

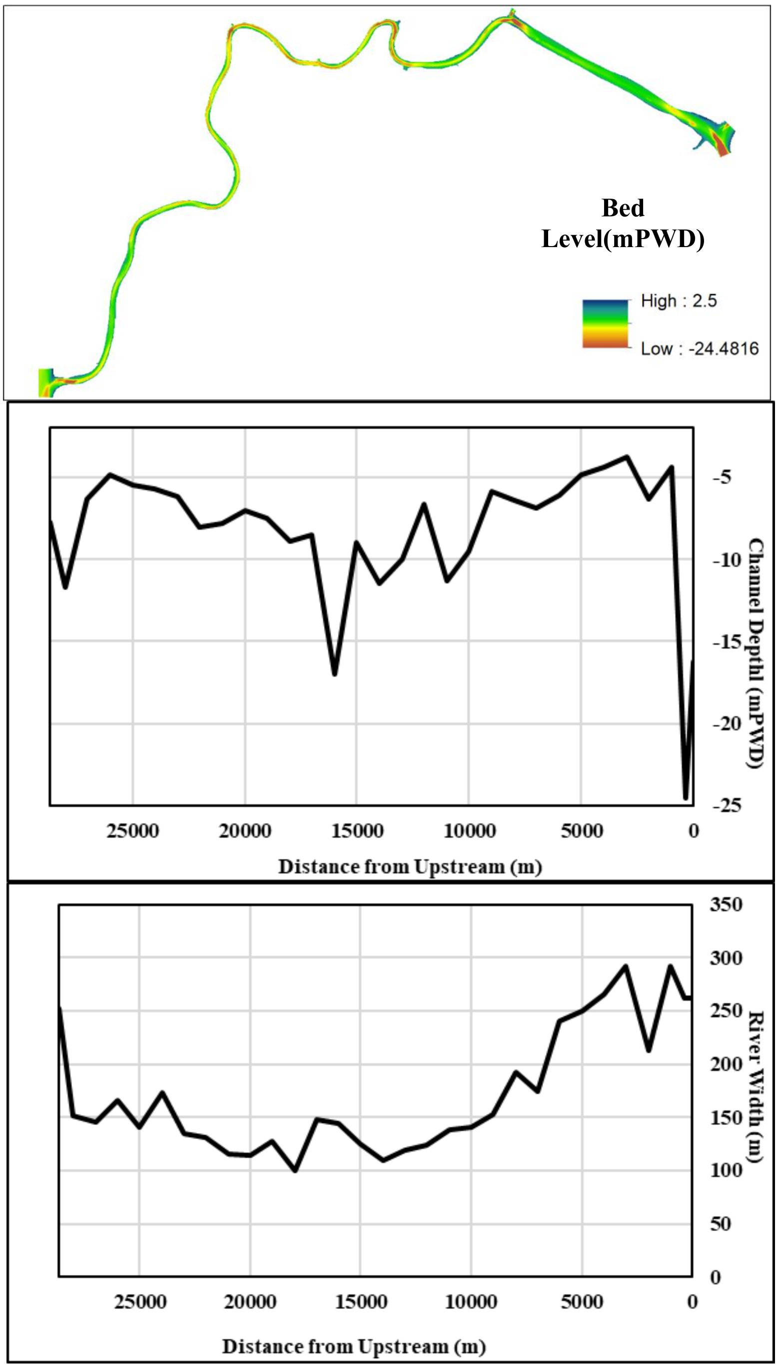

Figure 12: a) Contour map of river bed, b) Depth along thalweg line, c) Depth variation

3.3 HYDRODYNAMIC ANALYSIS

3.3.1 Tidal Range and Tidal Damping

The river system exhibits clear tidal damping, characterized by a gradual reduction of tidal energy in the upstream direction (Figure 13). This damping effect is more pronounced during the Low-Flow Season (LFS), when reduced freshwater discharge limits tidal propagation, resulting in lower damping factors ranging from 0.81 to 0.87. In contrast, during the High-Flow Season (HFS), damping is weaker, with values between 0.91 and 1, indicating greater tidal penetration upstream. Both HEC-RAS and Delft3D simulations show consistent damping behavior across seasons, demonstrating the reliability of the modeled tidal response.

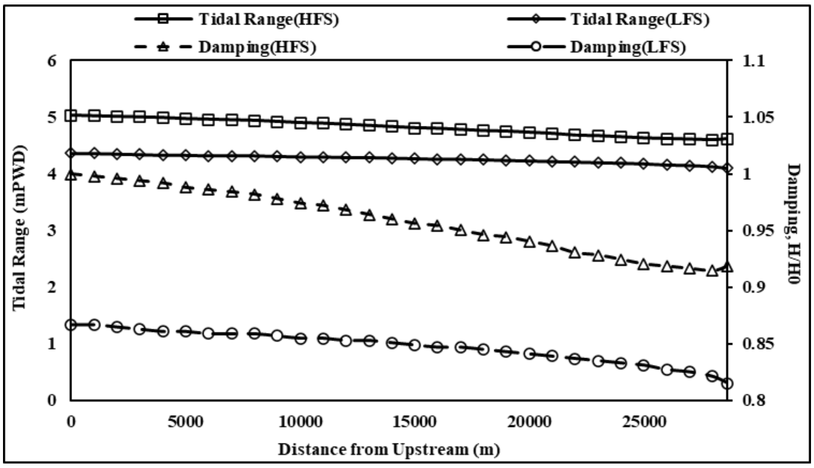

(a)

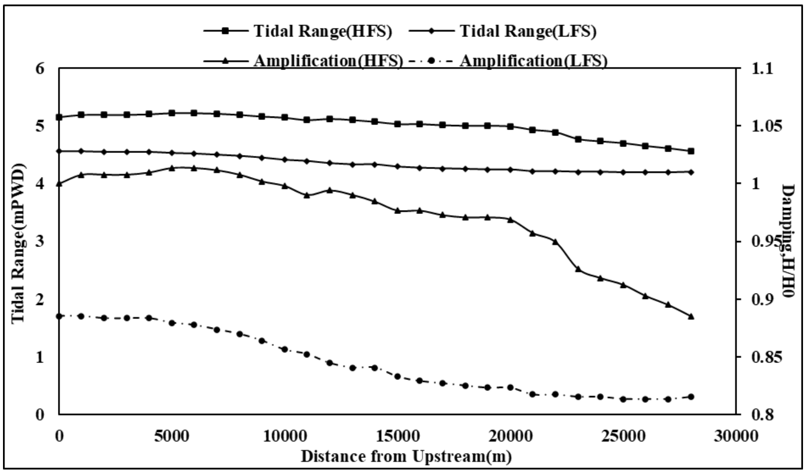

(b)

Figure 13: Tidal Range and Tidal Damping (a) HEC-RAS (b) Delft3D

3.3.2 Water Level

The Mongla River is semi-diurnal, experiencing two high and two low tides daily. The interval between consecutive tides is approximately 12 hours at both Doratana and Pussur River Outfall (Figure 14). The tidal phase difference between the two locations is generally about 2.5 hours, indicating delayed tidal propagation upstream due to channel friction, geometric convergence, and energy dissipation along the river. During the High-Flow Spring Tide (HFS-Spring), this phase lag reduces to approximately 2 hours, reflecting stronger tidal forcing and increased tidal prism, which enhance wave celerity and allow the tidal signal to propagate more rapidly upstream. The associated water level drop of 0.3–0.9 m between the two locations highlights the combined effects of tidal damping and channel resistance, with larger gradients occurring during energetic tidal conditions (Figures 15–18). A decrease in water level at Doratana is consistently associated with a downstream reduction in tidal elevations, indicating progressive tidal damping along the river reach. Peak water levels decline from approximately 3.93 mPWD at the upstream location to 3.46 mPWD downstream, reflecting energy loss due to bed friction, channel irregularities, and geometric constraints. This attenuation of tidal amplitude highlights the resistance imposed by the river morphology and emphasizes the dominance of frictional dissipation over tidal amplification within the study reach, particularly during periods of reduced discharge.

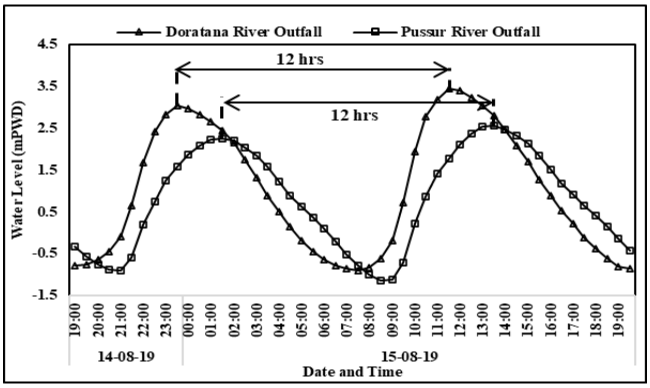

Figure 14: Tide Interval

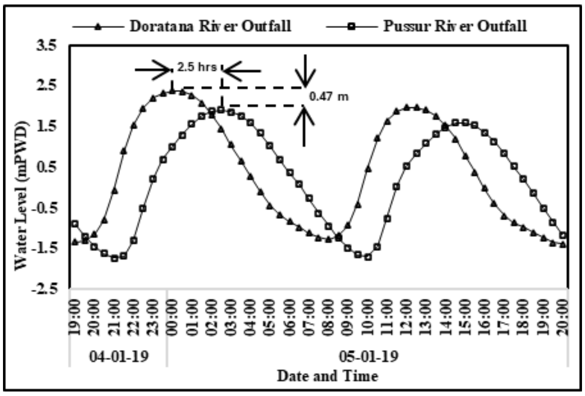

Figure 15: Phase Shift for LFS (Spring Tide)

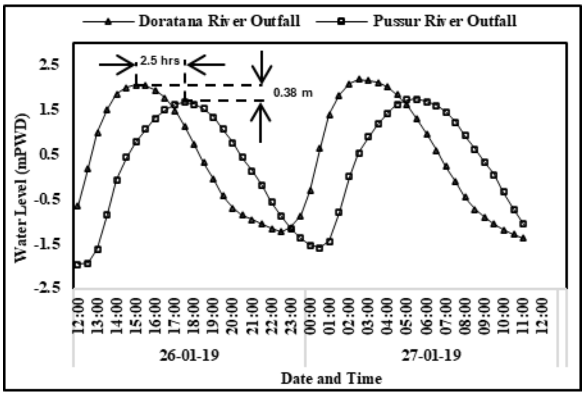

Figure 16: Phase Shift for LFS (Neap Tide)

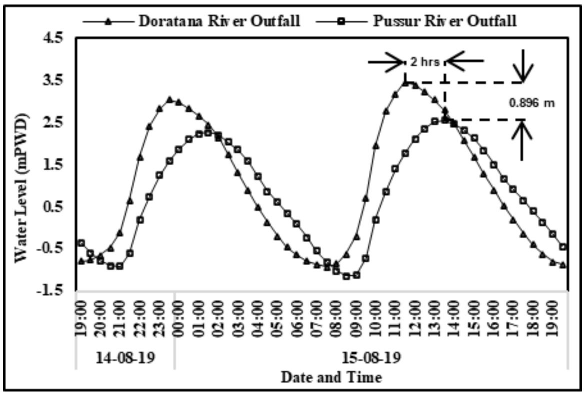

Figure 17: Phase Shift for HFS (Spring Tide)

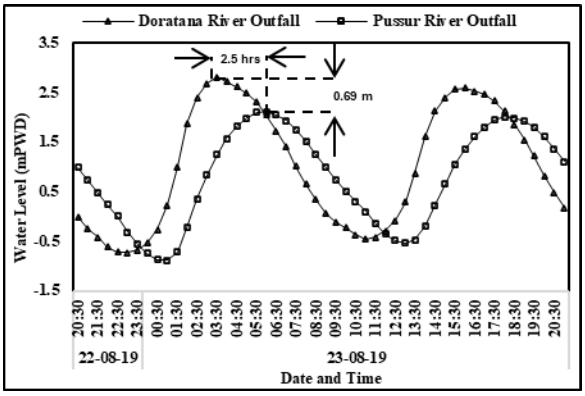

Figure 18: Phase Shift for HFS (Neap Tide)

4. CONCLUSIONS

The hydrodynamic analysis of the Mongla River reveals a strongly tide-dominated system governed by tidal propagation, velocity distribution, and seasonal discharge variability. Tidal damping and a 2–2.5-hour phase shift indicate progressive energy dissipation toward the upstream reach, while a velocity convergence zone near chainage 11 km promotes sediment deposition. Higher velocities during high-flow spring tides enhance bed scouring, whereas the dominance of flood tides favors sediment accumulation, posing persistent challenges to navigability. Comparative results with Delft3D demonstrate strong consistency, confirming the reliability of HEC-RAS 2D for simulating tidal river dynamics. Despite these insights, the study has certain limitations. The model does not explicitly simulate sediment transport and morphological evolution, and its performance is reduced during extreme low-flow conditions when partial channel drying occurs. Additionally, the analysis is based on a single year of hydrological data, which may not fully capture interannual variability or long-term trends influenced by climate change and upstream interventions.

Future research should incorporate coupled hydrodynamic–sediment transport modeling to quantify erosion and deposition processes more explicitly. Extending simulations over multiple years, integrating climate-driven sea-level rise scenarios, and assessing the impacts of river training and dredging strategies would further strengthen management applications. Such advancements would enhance the predictive capability of numerical models and support sustainable navigation, sediment management, and ecosystem conservation in the Mongla River and similar tidal river systems.

DECLARATION OF USE OF AI

The authors accept the fact that the tools of artificial intelligence were used to refine language and make the texts clearer. The authors formulated the scientific material, data review, result description, and conclusions, and thus they take full responsibility for the accuracy, novelty, and integrity of the paper.

REFERENCES

Ali, M. S. (2008). Model refinement of unsteady RANS and its practical applications in the field of hydraulic engineering, PhD Thesis, Kyoto University, Japan (https://doi.org/10.14989/doctor.k14139).

Rahman, M. M., Ahsan, M., Hore, S. K., Sarker, M. H., & Hossain, A. T. M. K. (2013). *Assessing the causes of deterioration of the Mongla-Ghasiakhali navigation route for restoration of navigability*. International Conference on Climate Change Impact and Adaptation (I3CIA-2013), Center for Climate Change and Sustainability Research, DUET, Gazipur, Bangladesh.

Hoitink, A. J. F., & Jay, D. A. (2016). Tidal river dynamics: Implications for deltas. *Reviews of Geophysics, 54*(1), 240–272. https://doi.org/10.1002/2015RG000507

Hoitink, A. J. F., Wang, Z. B., Vermeulen, B., Huismans, Y., & Kästner, K. (2017). Tidal controls on river delta morphology. *Nature Geoscience, 10*(9), 637-645. https://doi.org/10.1038/NGEO3000

Savant, G., & McAlpin, T. O. (2014). Tidal hydrodynamics in the Lower Columbia River estuary through depth averaged adaptive hydraulics modeling. *Journal of Engineering, 2014*, 1–12. https://doi.org/10.1155/2014/416914

Mahavadi, T. F., Seiffert, R., Kelln, J., & Fröhle, P. (2024). Effects of sea level rise and tidal flat growth on tidal dynamics and geometry of the Elbe estuary. *Ocean Science, 20*(2), 369–388. https://doi.org/10.5194/os-20-369-2024

Rahman, M., & Ali, M. S. (2018). Hydrological characteristics of Pussur River and its navigability. *Proceedings of the 4th International Conference on Civil Engineering for Sustainable Development (ICCESD-2018)*, 9–11 February, Khulna, Bangladesh. Mongla Port Authority.

Alam, R., Islam, M. S., Hasib, M. R., & Khan, M. Z. H. (2014). Characteristics of hydrodynamic processes in the Meghna estuary due to dynamic whirl action. *IOSR j. eng*, *4*(06), 39-50.

Kabir, S. M. I., & Ali, M. M. (2017). *Hydrodynamic and Morphological Simulation of Karnafuli River Using CCHE2D Model.* 6th International Conference on Water & Flood Management (ICWFM-2017).

Samir, F. (2024). Evaluate the numerical models' performance in the Nile River. ISH Journal of Hydraulic Engineering, 30(5), 696-704.

Muñoz, D. F., Yin, D., Bakhtyar, R., Moftakhari, H., Xue, Z., Mandli, K., & Ferreira, C. (2022). Inter-model comparison of Delft3D-FM and 2D HEC-RAS for total water level prediction in coastal to inland transition zones. *JAWRA Journal of the American Water Resources Association*, *58*(1), 34-49.

Rahman, M., & Ali, M. S. (2024). Drivers of tidal flow variability in the Pussur fluvial estuary: A numerical study by HEC-RAS. Heliyon, 10(4), e25662.